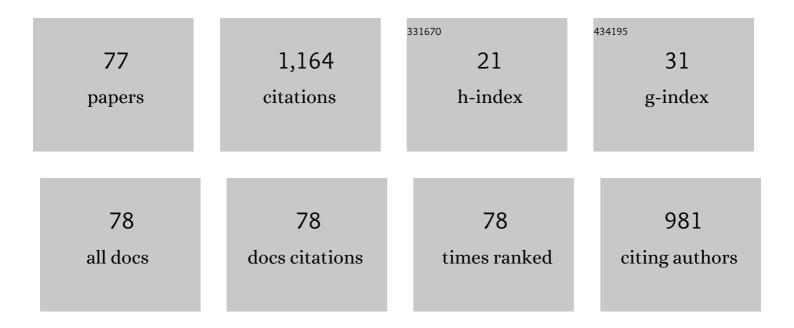
Danuta StrÃ³Å¹/₄

List of Publications by Year in descending order

Source: https://exaly.com/author-pdf/2016035/publications.pdf Version: 2024-02-01



Πλημιτά ςτρδ3Δ14

#	Article	IF	CITATIONS
1	Sonochemical preparation of SbSI gel. Ultrasonics Sonochemistry, 2008, 15, 709-716.	8.2	77
2	Fate of neutral-charged gold nanoparticles in the roots of the Hordeum vulgare L. cultivar Karat. Scientific Reports, 2017, 7, 3014.	3.3	56
3	Effect of Nanoparticles Surface Charge on the Arabidopsis thaliana (L.) Roots Development and Their Movement into the Root Cells and Protoplasts. International Journal of Molecular Sciences, 2019, 20, 1650.	4.1	50
4	Fabrication and characterization of SbSI gel for humidity sensors. Sensors and Actuators A: Physical, 2014, 210, 119-130.	4.1	46
5	Effect of early stages of precipitation and recovery on the multi-step transformation in deformed and annealed near-equiatomic NiTi alloy. Scripta Materialia, 2003, 48, 571-576.	5.2	44
6	Effect of ageing on martensitic transformation in NiTi shape memory alloy. Journal of Materials Science, 1988, 23, 4127-4131.	3.7	39
7	Ferroelectric properties of ultrasonochemically prepared SbSI ethanogel. Ultrasonics Sonochemistry, 2009, 16, 398-401.	8.2	37
8	Effect of thermal cycling on as-quenched and aged nickel-rich Ni-Ti alloy. Journal of Materials Science, 1991, 26, 1741-1748.	3.7	35
9	Two-stage R phase transformation in a cold-rolled and annealed Ti?50.6at.%Ni alloy. Scripta Materialia, 2005, 52, 757-760.	5.2	34
10	Novel piezoelectric paper based on SbSI nanowires. Cellulose, 2018, 25, 7-15.	4.9	32
11	A Ferroelectric-Photovoltaic Effect in SbSI Nanowires. Nanomaterials, 2019, 9, 580.	4.1	31
12	XPS analysis of sonochemically prepared SbSI ethanogel. Applied Surface Science, 2009, 255, 7689-7694.	6.1	30
13	The microstructure of erbium–ytterbium co-doped oxyfluoride glass–ceramic optical fibers. Optical Materials, 2012, 34, 944-950.	3.6	30
14	Diverse influence of nanoparticles on plant growth with a particular emphasis on crop plants. Acta Agrobotanica, 2016, 69, .	1.0	30
15	TEM studies of plasma nitrided austenitic stainless steel. Journal of Microscopy, 2010, 237, 227-231.	1.8	29
16	Unique chromoplast organisation and carotenoid gene expression in carotenoid-rich carrot callus. Planta, 2018, 248, 1455-1471.	3.2	28
17	Ferroelectric SbSI nanowires for ammonia detection at a low temperature. Talanta, 2018, 189, 225-232.	5.5	27
18	Influence of humidity on impedance of SbSI gel. Sensors and Actuators A: Physical, 2012, 183, 34-42.	4.1	26

#	Article	IF	CITATIONS
19	Sonochemical preparation of SbSel gel. Ultrasonics Sonochemistry, 2009, 16, 546-551.	8.2	24
20	Sonochemical preparation of SbS1â^'Se I nanowires. Ultrasonics Sonochemistry, 2010, 17, 487-493.	8.2	23
21	Preparation and Characterization of Nitinol Bone Staples for Cranio-Maxillofacial Surgery. Journal of Materials Engineering and Performance, 2012, 21, 2650-2656.	2.5	23
22	Quantum efficiency coefficient for photogeneration of carriers in SbSI nanowires. Optical Materials, 2013, 35, 2208-2216.	3.6	21
23	Fast and Efficient Piezo/Photocatalytic Removal of Methyl Orange Using SbSI Nanowires. Materials, 2020, 13, 4803.	2.9	21
24	Infrared spectroscopy of ferroelectric nanowires of antimony sulfoiodide. Infrared Physics and Technology, 2008, 51, 307-315.	2.9	20
25	The development of a hairless phenotype in barley roots treated with gold nanoparticles is accompanied by changes in the symplasmic communication. Scientific Reports, 2019, 9, 4724.	3.3	20
26	A new hybrid piezo/triboelectric SbSel nanogenerator. Energy, 2022, 238, 122048.	8.8	20
27	SbSI nanowires for ferroelectric generators operating under shock pressure. Materials Letters, 2016, 180, 15-18.	2.6	19
28	Using of sonochemically prepared SbSI for electrospun nanofibers. Ultrasonics Sonochemistry, 2017, 38, 544-552.	8.2	19
29	Sonochemical growth of antimony sulfoiodide in multiwalled carbon nanotube. Ultrasonics Sonochemistry, 2009, 16, 800-804.	8.2	18
30	A simple route for manufacture of photovoltaic devices based on chalcohalide nanowires. Applied Surface Science, 2020, 517, 146138.	6.1	18
31	Electrochemical Formation of Second Generation TiO2 Nanotubes on Ti13Nb13Zr Alloy for Biomedical Applications. Acta Physica Polonica A, 2016, 130, 1079-1080.	0.5	17
32	Sonochemical growth of antimony selenoiodide in multiwalled carbon nanotube. Ultrasonics Sonochemistry, 2012, 19, 179-185.	8.2	16
33	Influence of the solvent on ultrasonically produced SbSI nanowires. Ultrasonics Sonochemistry, 2009, 16, 537-545.	8.2	15
34	Nanogenerator for dynamic stimuli detection and mechanical energy harvesting based on compressed SbSel nanowires. Energy, 2020, 212, 118717.	8.8	15
35	Effect of Internal Strain on Martensitic Transformations in NiTi Shape Memory Alloys. Materials Transactions, 2011, 52, 358-363.	1.2	14
36	Sonochemical preparation of antimony subiodide. Ultrasonics Sonochemistry, 2010, 17, 219-227.	8.2	13

#	Article	IF	CITATIONS
37	Microstructure, Phase Transformations, and Properties of Hot-Extruded Ni-Rich NiTi Shape Memory Alloy. Journal of Materials Engineering and Performance, 2014, 23, 2362-2367.	2.5	13
38	Influence of Molybdenum on the Microstructure, Mechanical Properties and Corrosion Resistance of Ti20Ta20Nb20(ZrHf)20â^'xMox (Where: x = 0, 5, 10, 15, 20) High Entropy Alloys. Materials, 2022, 15, 393.	2.9	11
39	Sonochemical growth of nanomaterials in carbon nanotube. Ultrasonics, 2018, 83, 179-187.	3.9	10
40	Extruded Rods with <001> Axial Texture of Polycrystalline Ni-Mn-Ga Alloys. Materials Science Forum, 0, 635, 189-194.	0.3	9
41	Structure and Properties of NiTi Shape Memory Alloy after Cold Rolling in Martensitic State. Acta Physica Polonica A, 2016, 130, 1081-1084.	O.5	9
42	TEM studies of the R-phase transformation in a NiTi shape memory alloy after thermo-mechanical treatment. Materials Chemistry and Physics, 2003, 81, 460-462.	4.0	8
43	The Microstructure of Annealed Galfan Coating on Steel Substrate. Archives of Metallurgy and Materials, 2012, 57, 517.	0.6	8
44	Influence of γ-Fe precipitates on physical and mechanical properties of Cu–Fe alloys. Metals Technology, 1980, 7, 248-251.	0.3	7
45	Structure and Properties of Cold-Worked and Annealed Ti-Ni-Co Shape Memory Wires Designed for Medical Application. Solid State Phenomena, 0, 163, 118-122.	0.3	6
46	Martensite transformation bands studied in TiNi shape memory alloy by infrared and acoustic emission techniques. Metallic Materials, 2013, 50, 309-318.	0.3	6
47	Transmission electron microscopy analysis of phase separation in GaInAsSb films grown on GaSb substrate. Journal of Microscopy, 2006, 224, 121-124.	1.8	5
48	Studies of the R-phase transformation in a Ti–51at.%Ni alloy by transmission electron microscopy. Scripta Materialia, 2002, 47, 363-369.	5.2	4
49	Studies of NiTi Shape Memory Alloy after Severe Plastic Deformation. Solid State Phenomena, 0, 163, 137-140.	0.3	4
50	Hot Extrusion of Ni-Based Polycrystalline Ferromagnetic Shape Memory Alloys. Solid State Phenomena, 0, 203-204, 306-309.	0.3	4
51	Microstructure and Mechanical Properties of Co-Cr-Mo-Si-Y-Zr High Entropy Alloy. Metals, 2020, 10, 1456.	2.3	4
52	NiTi Shape Memory Marformed Alloy Studied by Electron Beam Precession TEM Orientation Mapping Method. Acta Physica Polonica A, 2017, 131, 1307-1311.	0.5	4
53	Instabilities in crystallization and magnetic behavior of Fe–Si–B amorphous alloys. Materials Research Bulletin, 2004, 39, 231-236.	5.2	3
54	Using of sonochemically prepared components for vapor phase growing of SbI3·3S8. Ultrasonics Sonochemistry, 2010, 17, 892-901.	8.2	3

#	Article	IF	CITATIONS
55	Optical properties of nanocomposite fibrous polymer mats containing SbSel nanowires. Optical Materials, 2018, 84, 383-388.	3.6	3
56	Precession Electron Diffraction Studies of SrxBa1-xNb2O6 and CaxBa1-xNb2O6 Single Crystals. Acta Physica Polonica A, 2016, 130, 830-832.	0.5	3
57	Carbon Coatings onto Shape Memory Alloys. Journal of Wide Bandgap Materials, 2001, 8, 189-194.	0.1	2
58	Structure of Antimony Sulfoiodide Ultrasonically Prepared in Carbon Nanotubes. Solid State Phenomena, 2010, 163, 88-92.	0.3	2
59	Structure and Properties of NiTi Shape Memory Alloys after Severe Plastic Deformation. Materials Science Forum, 0, 738-739, 501-505.	0.3	2
60	The Structure and Properties Formation of the NiTi Shape Memory Rods after Hot Rotary Forging. Key Engineering Materials, 2016, 687, 11-18.	0.4	2
61	The crystallization kinetics of Er/Yb co-doped oxyfluoride glasses. Proceedings of SPIE, 2017, , .	0.8	2
62	Martensitic Transformation in Nanostructured NiTi Alloy Studied by X-ray Diffraction <i>In-Situ</i> Heating. Materials Transactions, 2019, 60, 708-713.	1.2	2
63	Analysis of amorphous regions in severely marformed NiTi shape memory alloy. International Journal of Materials Research, 2019, 110, 18-23.	0.3	2
64	Interfacial Polarization Phenomena in Compressed Nanowires of SbSI. Materials, 2022, 15, 1543.	2.9	2
65	On the structured imperfections of bulk GaSb using high resolution transmission electron microscopy. Micron, 2009, 40, 6-10.	2.2	1
66	Structure and Functional Properties of Microcrystalline NiTi Alloy after Severe Deformation and Subsequent Annealing. Materials Science Forum, 2011, 674, 53-60.	0.3	1
67	Nanotexture Studies of NiTi Shape Memory Alloy after Severe Plastic Deformation with the Use of TEM. Solid State Phenomena, 2012, 186, 90-93.	0.3	1
68	Structure and Phase Transformation in Ni-Co-Mn-In Ferromagnetic Shape Memory Alloys. Solid State Phenomena, 0, 203-204, 240-245.	0.3	1
69	Properties of Sonochemically Prepared CulnxGa1-xS2and CulnxGa1-xSe2. Acta Physica Polonica A, 2014, 126, 1107-1109.	0.5	1
70	FOURIER SPECTROSCOPY OF IMAGES IN MATERIAL SCIENCE. , 2004, , .		0
71	TEM Study of Ni-Mn-Co-In Ferromagnetic Shape Memory Alloys. Solid State Phenomena, 0, 186, 271-274.	0.3	0
72	Microstructural Evolution and Corrosion Behavior of Carburized α-Fe Plates by Glucose. Solid State Phenomena, 2013, 203-204, 94-98.	0.3	0

#	Article	IF	CITATIONS
73	Structure and Properties of Ni-Rich Shape Memory Alloy Subjected to Severe Deformation and Annealing. Solid State Phenomena, 0, 203-204, 339-342.	0.3	0
74	Microstructural Studies of NiCoMnIn Magnetic Shape Memory Ribbons. Materials Science Forum, 0, 738-739, 436-440.	0.3	0
75	Characterization of As-Cast Single-Crystal CMSX-4 Superalloy Turbine Blades. Solid State Phenomena, 2013, 203-204, 173-176.	0.3	Ο
76	Electron Diffraction Reinvestigation of CdCr ₂ Se ₄ and ZnCr _{2-x} V _x Se ₄ Spinel Structures. Solid State Phenomena, 0, 203-204, 262-265.	0.3	0
77	The Structure and Shape Memory of the Hot Extruded NiTi Alloy. Key Engineering Materials, 2016, 687, 19-24.	0.4	0